

# BLIND SOURCE SEPARATION FROM MULTI-CHANNEL OBSERVATIONS WITH CHANNEL-VARIANT SPATIAL RESOLUTIONS

Koray Kayabol<sup>1,\*</sup>, Emanuele Salerno<sup>1</sup>, Jose Luis Sanz<sup>2</sup>, Diego Herranz<sup>2</sup> and Ercan E. Kuruoglu<sup>1</sup>

<sup>1</sup>ISTI, CNR, via G. Moruzzi 1, 56124, Pisa, Italy,  
{koray.kayabol, emaele.salerno, ercan.kuruoglu,}@isti.cnr.it,

<sup>2</sup>IFCA, University of Cantabria, Avda. Los Castros s/n 39005, Santander, Spain  
{sanz, herranz}@ifca.unican.es

## ABSTRACT

We propose a Bayesian method for separation and reconstruction of multiple source images from multi-channel observations with different resolutions and sizes. We reconstruct the sources by exploiting each observation channel at its exact resolution and size. The source maps are estimated by sampling the posteriors through a Monte Carlo scheme driven by an adaptive Langevin sampler. We use the  $t$ -distribution as prior image model. All the parameters of the posterior distribution are estimated iteratively along the algorithm. We experimented the proposed technique with the simulated astrophysical observations. These data are normally characterized by their channel-variant spatial resolution. Unlike most of the spatial-domain separation methods proposed so far, our strategy allows us to exploit each channel map at its exact resolution and size.

## 1. INTRODUCTION

In this study, we focus on the separation of source images from multi-channel blurred and noisy observations with channel-variant spatial resolutions. We face this kind of problem in astrophysical component inference from multi-channel observations. The resolutions of the observed channel maps are generally different, since the aperture of the telescope beam depends on frequency. Because of this physical restriction, for low resolution channel maps, less number of pixels than the the high resolution channel maps is needed. If the image sizes are different in observations, the most simple and intuitive procedure that can be applied is to interpolate the low resolution channels maps or decimate the high resolution channels maps to equal the size of all maps. However, data interpolation and decimation correlate the white noise and convert it to colored noise. The source separation for channel-variant spatial resolution and convolutional mixture case with equal sized observations has been taken into account in [1] to estimate the parametric mixing matrix and the power spectrums of the sources in the spatial frequency domain. In order to deal with different sized observation images, we propose a Bayesian formulation of the problem in the pixel domain and find the source maps by a recently developed Monte Carlo technique for image processing, namely the Langevin Sampler [2].

Image reconstruction from multi-channel low-resolution observations without mixing is a high-resolution and super-resolution image reconstruction problem. The pioneer works on super-resolution can be found in [3] and [4]. Super-resolution has been then used in video processing to improve the resolution of a video by using multiple low-resolution frames [5], [6]. Schultz and Stevenson have proposed a Bayesian approach to super-resolution [7], using the Maximum-a-Posteriori (MAP) estimation with Markov Random Field (MRF) prior. A study on improving the resolution of the hyper-spectral and astronomical images are found in [8] and [9] respectively. The studies in [10] and [11] summarize the super-resolution problem. We define our low-resolution observation model according to the one used in super-resolution [7].

In Blind Source Separation (BSS), the aim is to separate multiple sources from mixed observations when the mixture coefficients are not known. To solve the Bayesian source separation problem without incurring in smoothing artifacts, Monte Carlo methods based on drawing random samples from posterior densities seem a viable approach [12]. In this study, we propose to improve the efficiency of the standard Metropolis random-walk sampling scheme by producing the proposal samples in parallel. To this end, we resort to the Langevin stochastic equation [13], [14], [2]. The proposed samples are accepted or rejected by the usual Metropolis-Hastings scheme.

Bayesian image separation has been investigated in different studies [15], [12], [2]. In [2], the  $t$ -distribution is used as a prior to model the edge images, since it is a good statistical model for data ranging from broad-tailed to normally distributed. The  $t$ -distribution is a member of the Scale Mixtures of Gaussians (SMGs) family. The Bayesian framework is also capable of full optimization of all the parameters. In the parameter estimation side of the study, we prefer to use SMG mixture definition of the  $t$ -distribution over an integral. Since we use the integral form of the  $t$ -distribution, we exploit the Expectation-Maximization (EM) method for estimation of its parameters. We also optimize the discrete time step of the Langevin equation adaptively along the iterations. The algorithms have been tested on simulated astrophysical images, relevant to the PLANCK project [18].

In Section 2, the problem definition is given in a Bayesian framework. The simulation results are presented in Section 3 and interpreted in Section 4.

\* This work is supported by the Italian Space Agency research program on cosmology and fundamental physics. Koray Kayabol is also supported by the International Center for Theoretical Physics, Trieste, Italy, Training and Research in Italian Laboratories program. Partially supported by CNR-CSIC bilateral project- "Astrophysical data analysis using nonstationary signal processing".

## 2. BAYESIAN SOURCE SEPARATION AND HIGH RESOLUTION RECONSTRUCTION

We assume that  $K$  observed images,  $y_k, k \in \{1, \dots, K\}$ , are linear combinations of  $L$  source images,  $s_l, l \in \{1, \dots, L\}$ . Let the  $k$ -th observed image be denoted by  $y_k$ , where  $i \in \{1, 2, \dots, M\}$  is the lexicographically ordered pixel index. Similarly,  $s_{l,i}$ , with  $i \in \{1, 2, \dots, N\}$  and  $N \geq M$ , denotes the  $N$ -pixel representation of the  $l$ -th source image. If the effect of the telescope is taken into account and by denoting  $s_l$  and  $y_k$  as the vector representations of source and observation images, respectively, then the observation model can be written as

$$\mathbf{y}_k = \mathbf{B}_k \mathbf{H}_k \sum_{l=1}^L a_{k,l} \mathbf{s}_l + \mathbf{n}_k \quad (1)$$

where  $\mathbf{H}_k$  is the Toeplitz matrix representation of the point spread function (psf) in the  $k$ -th observation channel, matrix  $\mathbf{B}_k$  is an  $M \times N$  down-sampling matrix, which becomes the  $N \times N$  identity  $\mathbf{I}_N$  when one of the highest-resolution maps is available at the  $k$ -th channel (i.e., when  $M = N$ ) and  $a_{k,l}$  is the mixing coefficient. For example, to convert a  $3 \times 3$  image to  $2 \times 2$  one, we construct the down-sampling matrix such as

$$\mathbf{B} = \begin{bmatrix} 1 & 0 & 0 & | & 0 & 0 & 0 & | & 0 & 0 & 0 \\ 0 & 0 & 1 & | & 0 & 0 & 0 & | & 0 & 0 & 0 \\ 0 & 0 & 0 & | & 0 & 0 & 0 & | & 1 & 0 & 0 \\ 0 & 0 & 0 & | & 0 & 0 & 0 & | & 0 & 0 & 1 \end{bmatrix} \quad (2)$$

We do not specify the structure of  $\mathbf{B}_k$ , but interested readers can find it in [10] and [11]. We use this model to connect the high-resolution sources to the low resolution observations. It has also the useful property that while  $\mathbf{B}_k \mathbf{H}_k$  is the smoothing and the down-sampling operation, its transpose  $\mathbf{H}_k^T \mathbf{B}_k^T$  is the expansion and the interpolation operation. The image is first expanded by zero-padding matrix  $\mathbf{B}_k^T$  and then interpolated by the filter  $\mathbf{H}_k^T$ . The vector  $\mathbf{n}_k$  represents an iid zero-mean Gaussian noise with  $\Sigma = \sigma_k^2 \mathbf{I}_M$  covariance matrix. Although the noise is not homogeneous in the real astrophysical maps, noise variance is homogeneous within each considered sky patch.

### 2.1 Likelihood

Since the observation noise is assumed to be independent and identically distributed zero-mean Gaussian at each pixel, the likelihood is expressed as

$$p(\mathbf{y}_{1:K} | \mathbf{s}_{1:L}, \mathbf{A}) \propto \prod_{k=1}^K \exp \{ -W(\mathbf{s}_{1:L} | \mathbf{y}_k, \mathbf{A}, \sigma_k^2) \} \quad (3)$$

$$W(\mathbf{s}_{1:L} | \mathbf{y}_k, \mathbf{A}, \sigma_k^2) = \frac{\|(\mathbf{y}_k - \mathbf{B}_k \mathbf{H}_k \sum_{l=1}^L a_{k,l} \mathbf{s}_l)\|^2}{2\sigma_k^2} \quad (4)$$

where the mixing matrix  $\mathbf{A}$  contains all the mixing coefficients  $a_{k,l}$  introduced in (1). We assume uniform prior for  $a_{k,l}$ .

### 2.2 Source Model

In this paper, we use the image model previously proposed in [2]. For this purpose, we write an auto-regressive source model using the first order neighbors of the pixel in the direction  $d$ :

$$\mathbf{s}_l = \alpha_{l,d} \mathbf{G}_d \mathbf{s}_l + \mathbf{t}_{l,d} \quad (5)$$

where the maximum number of first order neighbors is 8 but we use only 4 neighbors,  $d \in \{1, \dots, 4\}$ , in the vertical and horizontal directions. Matrix  $\mathbf{G}_d$  is a linear one-pixel shift operator,  $\alpha_d$  is the regression coefficient and the regression error  $\mathbf{t}_{l,d}$  is an iid  $t$ -distributed zero-mean vector with degree of freedom parameter  $\beta_{l,d}$  and scale parameters  $\delta_{l,d}$ . The multivariate probability density function of an image modelled by a  $t$ -distribution can be written as

$$p(\mathbf{t}_{l,d} | \alpha_{l,d}, \beta_{l,d}, \delta_{l,d}) = \frac{\Gamma((N + \beta_{l,d})/2)}{\Gamma(\beta_{l,d}/2) (\pi \beta_{l,d} \delta_{l,d})^{N/2}} \times \left[ 1 + \frac{\phi_d(\mathbf{s}_l, \alpha_{l,d})}{\beta_{l,d} \delta_{l,d}} \right]^{-(N + \beta_{l,d})/2} \quad (6)$$

where  $\phi_d(\mathbf{s}_l, \alpha_{l,d}) = \|\mathbf{t}_{l,d}\|^2 = \|\mathbf{s}_l - \alpha_{l,d} \mathbf{G}_d \mathbf{s}_l\|^2$  and  $\Gamma(\cdot)$  is the Gamma function. We can write the density of  $s_l$  by using the image differentials in different directions, by assuming the directional independence, as

$$p(\mathbf{s}_l | \alpha_{l,d}, \beta_{l,d}, \delta_{l,d}) = \prod_{d=1}^4 p(\mathbf{t}_{l,d} | \alpha_{l,d}, \beta_{l,d}, \delta_{l,d}). \quad (7)$$

We assume uniform priors for  $\alpha_{l,d}$  and  $\delta_{l,d}$  and use non-informative Jeffrey's prior for  $\beta_{l,d}$ :  $\beta_{l,d} \sim 1/\beta_{l,d}$ .

### 2.3 Posteriors

To define the BSS problem in the Bayesian framework, the joint posterior density of all of the unknowns must be written.

$$p(\mathbf{s}_{1:L}, \mathbf{A}, \Theta | \mathbf{y}_{1:K}) \propto p(\mathbf{y}_{1:K} | \mathbf{s}_{1:L}, \mathbf{A}) p(\mathbf{s}_{1:L}, \mathbf{A}, \Theta) \quad (8)$$

where  $\Theta = \{\alpha_{1:L,1:4}, \beta_{1:L,1:4}, \delta_{1:L,1:4}\}$ ,  $p(\mathbf{y}_{1:K} | \mathbf{s}_{1:L}, \mathbf{A})$  is the likelihood and  $p(\mathbf{s}_{1:L}, \mathbf{A}, \Theta)$  is the joint prior density of unknowns. The joint prior can be factorized as  $p(\mathbf{s}_{1:L} | \alpha_{1:L,1:4}, \beta_{1:L,1:4}, \delta_{1:L,1:4}) p(\mathbf{A}) p(\beta_{1:L,1:4}) p(\delta_{1:L,1:4}) p(\alpha_{1:L,1:4})$ . Furthermore, since the sources are assumed to be independent, the joint probability density of the sources is also factorized as

$$p(\mathbf{s}_{1:L} | \Theta) = \prod_{l=1}^L p(\mathbf{s}_l | \Theta) \quad (9)$$

To estimate all unknowns, we write their conditional posteriors as

$$\begin{aligned} p(a_{k,l} | \mathbf{y}_{1:K}, \mathbf{s}_{1:L}, \mathbf{A}_{-a_{k,l}}, \Theta) &\propto p(\mathbf{y}_{1:K} | \mathbf{s}_{1:L}, \mathbf{A}) \\ p(\alpha_{l,d} | \mathbf{y}_{1:K}, \mathbf{s}_{1:L}, \mathbf{A}, \Theta_{-\alpha_{l,d}}) &\propto p(\mathbf{t}_{l,d} | \Theta) \\ p(\beta_{l,d} | \mathbf{y}_{1:K}, \mathbf{s}_{1:L}, \mathbf{A}, \Theta_{-\beta_{l,d}}) &\propto p(\mathbf{t}_{l,d} | \Theta) p(\beta_{l,d}) \\ p(\delta_{l,d} | \mathbf{y}_{1:K}, \mathbf{s}_{1:L}, \mathbf{A}, \Theta_{-\delta_{l,d}}) &\propto p(\mathbf{t}_{l,d} | \Theta) \\ p(\mathbf{s}_l | \mathbf{y}_{1:K}, \mathbf{s}_{(1:L)-l}, \mathbf{A}, \Theta) &\propto p(\mathbf{y}_{1:K} | \mathbf{s}_{1:L}, \mathbf{A}) p(\mathbf{s}_l | \Theta) \end{aligned} \quad (10)$$

where the “-variable” expressions in the subscripts denote the removal of that variable from the variable set.

The Maximum Likelihood (ML) estimations of the parameters  $\alpha_{l,d}$ ,  $\beta_{l,d}$  and  $\delta_{l,d}$  are obtained using an Expectation-Maximization (EM) method [2]. To estimate the source images, we use Langevin sampler, whose details are given in Section 2.4.

## 2.4 Astrophysical Map Estimation

In the classical Markov Chain Monte Carlo (MCMC) schemes, a random walk process is used to produce the proposal samples. Although random walk is simple, it affects adversely the convergence time. Instead of random walk, we use the Langevin stochastic equation, which exploits the gradient information of the energy function to produce a new proposal. Since the gradient directs the proposed samples towards the mode, the final sample set will mostly come from around the mode of the posterior. The Langevin equation used in this study is written as

$$\mathbf{s}_l^{k+1} = \mathbf{s}_l^k - \frac{1}{2} \mathbf{D}_l \mathbf{g}(\mathbf{s}_l^k) + \mathbf{D}_l^{\frac{1}{2}} \mathbf{w}_l \quad (11)$$

where the diagonal matrix  $\mathbf{D}_l^{\frac{1}{2}}$  contains the discrete time steps  $\tau_{l,n}$ ,  $n = 1 : N$ , so that, for the  $i$ th pixel, the diffusion coefficient is  $\mathbf{D}_l(n, n) = \tau_{l,n}^2$ . Matrix  $\mathbf{D}_l$  is referred to here as diffusion matrix. We determine it by taking the inverse of the diagonal of the Hessian matrix which is calculated through the energy function  $E(\mathbf{s}_l) = W(\mathbf{s}_{1:L}) + U(\mathbf{s}_l)$  where  $U(\mathbf{s}_l) = -\log p(\mathbf{s}_l | \alpha_{l,d}, \beta_{l,d}, \delta_{l,d})$  defined in (7).  $\mathbf{g}(\mathbf{s}_l^k)$  is the gradient of the energy  $E(\mathbf{s}_l)$  with respect to  $\mathbf{s}_l$  and is defined in Table 1.

Since the random variables for the image pixel intensities are produced in parallel by (11), this procedure is faster than the random walk adopted in [12]. The derivation details of the equation can be found in [2]. A similar form of Langevin equation is also found in [16] and [17].

The samples are produced by using this first order equation, and then they are tested in the Metropolis-Hastings scheme. The samples produced by (11) are applied to a Metropolis-Hastings scheme pixel-by-pixel. The acceptance probability of any proposed sample is defined as  $\min\{\varphi(s_{l,n}^{k+1}, s_{l,n}^k), 1\}$ , where

$$\varphi(s_{l,n}^{k+1}, s_{l,n}^k) \propto e^{-\Delta E(s_{l,n}^{k+1})} \frac{q(s_{l,n}^k | s_{l,n}^{k+1})}{q(s_{l,n}^{k+1} | s_{l,n}^k)} \quad (12)$$

where  $\Delta E(s_{l,n}^{k+1})$  is the energy difference between the proposed and current pixel.

The proposal density  $q(s_{l,n}^{k+1} | s_{l,n}^k)$  is obtained, from (11), as

$$\mathcal{N}\left(s_{l,n}^{k+1} | s_{l,n}^k + \frac{\tau_l^2}{2} \mathbf{g}(s_{l,n}^k), \tau_l^2\right) \quad (13)$$

The summary of the Metropolis-Hastings algorithm with Langevin proposal is given in in Table 1.

## 3. SIMULATION RESULTS

This section presents some astrophysical image separation results of the proposed method, compared to the corresponding results from other methods. The proposed method is denoted as ALS (Adaptive Langevin Sampler) and compares to two ad hoc methods. In both of the competitor methods, we apply an interpolation (IP) to the low resolution and small sized channels. It corresponds to the operation  $\mathbf{H}_k^T \mathbf{B}_k^T$ , but one can use any interpolation technique to perform interpolation. In the first competitor method, we apply the pre-estimated separation matrix to find LS solution. As a

Table 1: Metropolis-Hastings algorithm with Langevin proposal.  $u$ : uniform positive random number in the unit interval;  $\mathbf{z}$ : generated sample vector to be tried;  $\varphi(z_n, s_{l,n}^k)$ : acceptance ratio of the generated sample.

1.  $\mathbf{w}_l \sim \mathcal{N}(\mathbf{w}_l | 0, \mathbf{I})$
2.  $\overline{\mathbf{H}}(\mathbf{s}_l^k) \leftarrow \text{diag}\{\mathbf{H}(\mathbf{s}_l)\}_{\mathbf{s}_l \leftarrow \mathbf{s}_l^k}$
3.  $\mathbf{D}_l \leftarrow 2[\overline{\mathbf{H}}(\mathbf{s}_l^k)]^{-1}$
4.  $\mathbf{g}(\mathbf{s}_l^k) \leftarrow [\nabla_{\mathbf{s}_l} E(\mathbf{s}_{1:L})]_{\mathbf{s}_{1:L} = \mathbf{s}_{1:L}^k}$
5. produce  $\mathbf{z} \leftarrow \mathbf{s}_l^k - \frac{1}{2} \mathbf{D}_l \mathbf{g}(\mathbf{s}_l^k) + \mathbf{D}_l^{\frac{1}{2}} \mathbf{w}_l$  from (11).
6. for all pixel  $n = 1, \dots, N$ 
  - (a) calculate  $\varphi(z_n, s_{l,n}^k)$
  - (b) if  $\varphi(z_n, s_{l,n}^k) \geq 1$  then  $s_{l,n}^{k+1} = z_n$   
else produce  $u \sim U(0, 1)$ .  
if  $u < \varphi(z_n, s_{l,n}^k)$  then  $s_{l,n}^{k+1} = z_n$ ,  
else  $s_{l,n}^{k+1} = s_{l,n}^k$
  - (c)  $n + 1 \leftarrow$  next pixel.

pre-estimation method, one can use Independent Component Analysis (ICA), Spectral Matching ICA (SMICA) or Fourier Domain Correlated Component Analysis (FDCCA) [1]. In the second competitor method, we first apply de-blurring (DB) and then find LS solution. For de-blurring, we use the Wiener filter with known psf and noise covariance. We call the competitor methods IP+LS and DB+IP+LS, respectively. We use the solution of IP+LS as initial value for our methods, so we call the proposed method as IP+LS+ALS. We also compare the results with those obtained from the channel invariant single resolution observations by ALS method. We have tested our algorithm on a sky patch that is located at (0,60) galactic coordinates. The observation images are generated by using a  $9 \times 3$  mixing matrix simulating nine images at frequencies 30, 44, 70, 100, 143, 217, 353, 545, and 857 GHz. In other words, we have  $K = 9$  observations and  $L = 3$  sources. Fig. 1 shows the observations in the patch considered. The size of the first three channel maps, 30, 44 and 70 GHz, is  $128 \times 128$ , whereas the others have size  $256 \times 256$ .

Fig. 2 shows the ground truth astrophysical source images and the estimated ones with IP+LS+ALS, IP+LS, ch. invar. IP+LS+ALS with channel invariant observations and ch. var. IP+DB+LS with channel variant observations. The mixed sources are CMB, synchrotron and dust maps, as simulated in preparation of the PLANCK mission of the European Space Agency (ESA) [18].

The Peak Signal-to-Inference Ratio (PSIR) is used as a numerical performance indicator. The PSIR values of the estimated maps are reported under each result in Fig. 2.

The PSIR values of ALS are over those of other methods. We can see from Fig. 2 that the IP+LS gives noisy and IP+DB+LS gives smoothed estimates, but the results of ALS are better than the others.

## 4. CONCLUSION

We have introduced a data model accounting for resolution and map size differences in the astrophysical source separation problem. We then solve this problem in a Bayesian

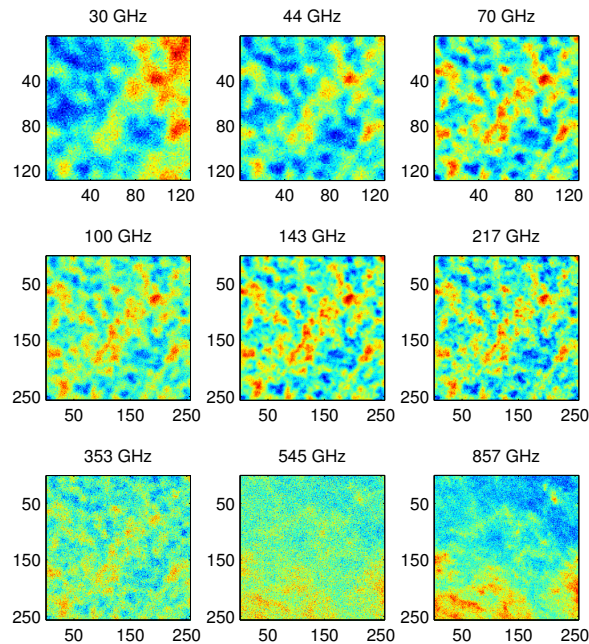


Figure 1: The blurred and noisy observations located at  $0^\circ$  longitude and  $60^\circ$  latitude. The first row: Low resolution  $128 \times 128$  channels. Second and third rows: High resolution  $256 \times 256$  channels.

framework by a Monte Carlo technique. The results show that our method outperforms two other strategies that do not take the proper resolutions and sizes into account. As part of our future work, we will evaluate the spatial resolutions that can be obtained in the source maps reconstructed by this technique, and explore the possibility of further improvements.

## 5. ACKNOWLEDGMENT

The authors would like to thank Anna Bonaldi, (INAF, Padova, Italy) and Bulent Sankur, (Bogazici University, Turkey) for their valuable discussions. The simulated maps are courtesy of the Planck working group on diffuse component separation (WG2.1).

## REFERENCES

- [1] L. Bedini and E. Salerno, "Extracting astrophysical sources from channel-dependent convolutional mixtures by correlated component analysis in the frequency domain," *Lec. Notes in Artificial Intell.*, vol. 4694, pp. 9–16, 2007.
- [2] K. Kayabol, E. E. Kuruoglu, J. L. Sanz, B. Sankur, E. Salerno, and D. Herranz, "Adaptive Langevin sampler for separation of  $t$ -distribution modelled astrophysical maps," *IEEE Trans. on Image Process.*, Feb. 2010, Accepted. [Online]. Available: [http://www.ieeexplore.ieee.org/xpls/abs\\_all.jsp?arnumber=5451169](http://www.ieeexplore.ieee.org/xpls/abs_all.jsp?arnumber=5451169)
- [3] R.W. Gerchberg, "Super-resolution through error energy reduction," *Optica Acta*, vol.21, no.9, pp. 709–720, 1974.
- [4] A. Papoulis, "A new algorithm in spectral analysis and band-limited extrapolation," *IEEE Trans. Circuits and Systems*, vol.22, no.9, pp. 735–742, 1975.
- [5] T. Y. Huang and R. Y. Tsay, "Multiple frame image restoration and registration," *Advances in Computer Vision and Image Process.*, vol. 1, pp. 317–339, 1984.
- [6] S. P. Kim, N. K. Bose, and H. M. Valenzuela, "Recursive reconstruction of high resolution image from noisy undersampled frames," *IEEE Trans. Acoust., Speech, Signal Process.*, vol. 38, pp. 1013–1027, 1990.
- [7] R. R. Schultz and R. L. Stevenson, "A Bayesian approach to image expansion for improved definition," *IEEE Trans. on Image Process.*, vol. 3, no. 3, pp. 233–242, 1994.
- [8] T. Akgun, Y. Altunbasak and R.M. Mersereau, "Super-resolution reconstruction of hyperspectral images," *IEEE Trans. on Image Process.*, vol. 14, no. 11, pp. 1860–1875, 2005.
- [9] A. Jalobeanu, J.A. Gutierrez and E. Slezak, "Multi-source data fusion and super-resolution from astronomical images," *Statistical Methodology*, vol. 5, pp. 361–372, 2008.
- [10] S. C. Park, M. K. Park, and M. G. Kang, "Superresolution image reconstruction: A technical overview," *IEEE Signal Process. Magazine*, vol. 20, no. 3, pp. 21–36, May 2003.
- [11] S. Farsiu, D. Robinson, M. Elad, and P. Milanfar, "Advances and challenges in super-resolution," *Int. J. Imaging Syst. Technol.*, vol. 14, pp. 47–57, 2004.
- [12] K. Kayabol, E. E. Kuruoglu, and B. Sankur, "Bayesian

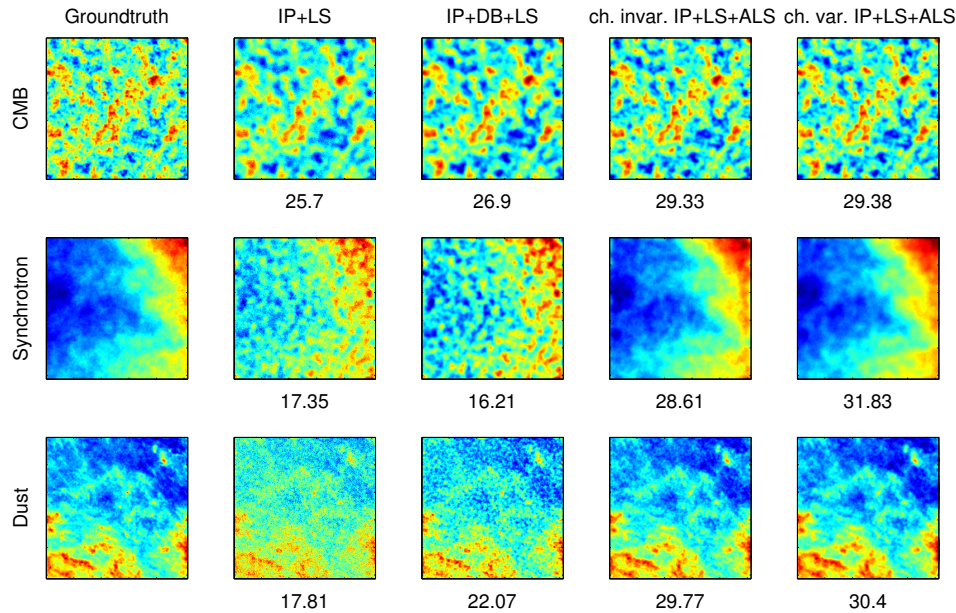


Figure 2: Reconstructed astrophysical maps from blurred and noisy observations by the IP+LS, IP+DB+LS, ch. invar. IP+LS+ALS and ch. var. IP+DB+LS methods. The location of the patch is  $0^\circ$  galactic longitude and  $60^\circ$  galactic latitude. The numbers under the reconstructed maps are the PSIR values in dB.

separation of images modelled with MRFs using MCMC,” *IEEE Trans. on Image Process.*, vol. 18, no. 5, pp. 982–994, 2009.

- [13] R.J. Rossky, J.D. Doll, and H.L. Friedman, “Brownian dynamics as a smart Monte Carlo simulation,” *J. Chem. Phys.*, vol. 69, pp. 4628–4633, 1978.
- [14] R.M. Neal, “Probabilistic inference using Markov chain Monte Carlo methods,” Tech. Rep. CRG-TR-93-1, Dept. Comp. Scien., University of Toronto”, Sep. 1993.
- [15] E. E. Kuruoglu, A. Tonazzini, and L. Bianchi, “Source separation in noisy astrophysical images modelled by Markov random fields,” in *Int. Conf. on Image Proc. ICIP’04*, pp. 24–27, Oct., 2004.
- [16] U. Grenander and M. I. Miller, “Representations of knowledge in complex systems (with discussion),” *J. R. Statist. Soc. B*”, vol. 56, pp. 549–603, 1994.
- [17] P. Dostert, Y. Efendiev, T. Y. Hou and W. Luo, “Coarse-gradient Langevin algorithms for dynamic data integration and uncertainty quantification,” *J. Comput. Phys.*”, vol. 217, pp. 123–142, 2006.
- [18] Planck Science Team, “PLANCK: The scientific programme,” *European Space Agency (ESA)*, 2005. [Online]. Available: <http://www.esa.int/SPECIALS/Planck/index.html>